



## Fatigue crack growth simulation in heterogeneous material using s-version FEM

Masanori Kikuchi<sup>a</sup>, Yoshitaka Wada<sup>b,\*</sup>, Yuichi Shintaku<sup>c</sup>, Kazuhiro Suga<sup>a</sup>, Yulong Li<sup>d</sup>

<sup>a</sup> Tokyo University of Science, 2641 Yamazaki, Noda, Chiba 278-8510, Japan

<sup>b</sup> Kinki University, 3-4-1 Kowakae, Higashiosaka, Osaka 577-8502, Japan

<sup>c</sup> Graduation School of Tokyo University of Science, 2641 Yamazaki, Noda, Chiba 278-8510, Japan

<sup>d</sup> Northwestern Polytechnical University, 127 Youyi Xilu, Xian, 710072 Shaanxi, PR China

### ARTICLE INFO

#### Article history:

Received 19 December 2012

Received in revised form 25 April 2013

Accepted 27 April 2013

Available online 16 May 2013

#### Keywords:

Fracture mechanics

Fatigue crack propagation

Heterogeneous material

s-FEM

### ABSTRACT

A fully automatic fatigue crack growth simulation system is developed using the s-version Finite Element Method (s-FEM). This system is extended to fractures in heterogeneous materials. In a heterogeneous material, the crack tip stress field has a mixed-mode condition, and the crack growth path is affected by inhomogeneous materials and mixed-mode conditions. Stress intensity factors (SIFs) in the mixed-mode condition are evaluated using the virtual crack closure method (VCCM). The criteria for the crack growth amount and crack growth path are based on these SIFs, and the growing crack configurations are obtained. At first, the basic problem is solved, and the results are compared with some results available in the literature. It is shown that this system gives an adequate accurate estimation of the SIFs. Then, two-dimensional fatigue crack growth problems are simulated using this system. The first example is a plate with an interface between hard and soft materials. The cracks tend to grow in soft materials through the interface. A second example is a plate with distributed hard inclusions. The crack takes a zig-zag path by propagating around the hard inclusions. In each case, the crack growth path changes in a complicated manner. Changes of the SIFs values are also shown and discussed.

© 2013 Elsevier Ltd. All rights reserved.

### 1. Introduction

Fatigue crack growth is important when dealing with the integrity of structures. To avoid catastrophic accidents, predictions of the crack growth path and residual fatigue life are key technologies. When fatigue crack growth occurs in complicated structures, these predictions meet serious difficulties. The Finite Element Method (FEM) is usually used for these predictions. Buchholz [1], Buchholz et al. [2] and Carpinteri et al. [3–5] simulated three-dimensional fatigue crack growth problems and compared them with experimental results. These studies successfully showed good agreement between the numerical simulation results and the experimental ones.

In the three-dimensional problem, fatigue cracks grow in a very complicated manner under the mixed-mode loading condition. In such a case, the re-meshing process becomes time-consuming work, and it has been a bottleneck for the application of FEM to fatigue crack growth problems.

Recently, several new techniques have been developed to overcome these difficulties. The element-free Galerkin method [6] was developed as a mesh-free technique and can be used to simulate the crack growth process [7]. X-FEM [8] is another kind of mesh-free crack growth technique. Nagashima et al. [9] simulated surface crack growth problems using this method. Superposition-FEM (s-FEM [10]) has been developed to make the re-meshing processes easy and it is able to predict complicated crack paths. Portela et al. [11] simulated surface crack growth problems using the dual boundary element method (Dual BEM).

The authors have developed a fully automatic fatigue crack growth simulation system [12] using s-FEM and applied it to three-dimensional surface crack problems, in order to evaluate the interaction of multiple surface cracks [13], and the crack closure effects of surface cracks [14]. The system is modified to manage residual stress field problems, and the stress corrosion cracking process is simulated [15]. An example of residual stress field is that generated by welding. In the heat-affected zone (HAZ), the grain size differs from those present in the other areas, and the mechanical properties differ from those of the base metals. For the evaluation of the stress corrosion cracking (SCC) and fatigue crack growth in such area, the changes in material properties should be considered. In s-FEM, local area is superpositioned onto global area. The meshes of local area and global area can be

\* Corresponding author. Tel.: +81 667212332

E-mail addresses: [kik@rs.noda.tus.ac.jp](mailto:kik@rs.noda.tus.ac.jp) (M. Kikuchi), [wada@mech.kindai.ac.jp](mailto:wada@mech.kindai.ac.jp) (Y. Wada), [shin@me.noda.tus.ac.jp](mailto:shin@me.noda.tus.ac.jp) (Y. Shintaku), [ksuga@rs.noda.tus.ac.jp](mailto:ksuga@rs.noda.tus.ac.jp) (K. Suga), [liyuloong@nwpu.edu.cn](mailto:liyuloong@nwpu.edu.cn) (Y. Li).

## Nomenclature

$\Omega$	area of the body
$\Omega^G$	global areas
$\Omega^L$	local areas
$\Gamma^{GL}$	boundary between the global areas and the local areas
$u_i^G$	displacement of the global areas
$u_i^L$	displacement of the local areas
$u_i$	displacement of the body
$[B^G]$	displacement–strain matrices defined in the global areas
$[B^L]$	displacement–strain matrices defined in the local areas
$[D^{GG}]$	stress–strain matrices described using the Young's modulus and Poisson's ratio in the global areas
$[D^{LL}]$	stress–strain matrices described using the Young's modulus and Poisson's ratio in the local areas
$[K^{GG}]$	stiffness matrices in the global areas
$[K^{LL}]$	stiffness matrices in the local areas
$[K^{GL}], [K^{LG}]$	stiffness matrices which express relationship between the local and global areas
$E, E_1, E_2$	Young's modulus
$\nu$	Poisson's ratio
$G_{12}, G_{23}, G_{32}$	shear modulus of anisotropic material
$\nu_{12}, \nu_{23}, \nu_{31}$	Poisson's ratio of anisotropic material
$P$	inner pressure

$a$	length of a crack in 2-dimension. Depth of a surface crack from surface in 3-dimension
$d$	distance between the boundary and the crack
$G_1, G_2$	shear modulus
$\Gamma$	ratio of $G_2$ to $G_1$
$G$	energy release rate
$h$	element size
$\alpha, \beta$	nodal points at the crack surface side
$A, B$	nodal points in the elements including crack tip
$u_i^{upper}, u_i^{lower}$	displacement along the $y'$ axis
$f_i, f_i^P$	equivalent nodal force
$K$	stress intensity factor
$F$	dimensionless stress intensity factor
$\sigma$	far field tensile loading stress
$da/dN$	crack propagation rate
$C, n$	material constants
$\Delta K_{eq}$	equivalent stress intensity factor range
$K_I, K_{II}, K_{III}$	stress intensity factor of modes I, II and III
$\Delta K_I, \Delta K_{II}, \Delta K_{III}$	stress intensity factor range of modes I, II and III
$\theta_0$	angle between local coordinate and crack surface
$\varphi_0$	crack propagation direction
$c$	crack length of the surface crack at the surface
$c_0$	initial crack length of the surface crack at the surface

independently defined. This feature can realize multiscale analysis including discontinuous structures like a crack. In actual s-FEM analysis, local meshes are re-meshed for the new crack configuration in each calculation step of the crack growth, and the local areas change shape in each calculation step. It seems difficult to change the material properties of a local mesh following the change in local mesh shape.

In this paper, such a problem is solved, and a crack growth simulation system for heterogeneous materials is developed. In the following, the new method is explained briefly. The numerical accuracy of the method is verified by comparison with the previous works [13,14]. Several practical problems are simulated in two-dimensional and three-dimensional stress fields, and the effect of the existence of an interface and changes in the material properties are studied and discussed.

## 2. Application of s-FEM to heterogeneous materials

S-FEM was originally proposed by Fish et al. [10]. As shown in Fig. 1, a structure with a crack is modeled with a global mesh and a local mesh. The global area  $\Omega^G$  (Fig. 1) does not include a crack, so a coarse mesh is used for the modeling of such an area. A crack is modeled in the local area  $\Omega^L$  (Fig. 1) using a fine mesh around the crack tip. The local area is superimposed on the global

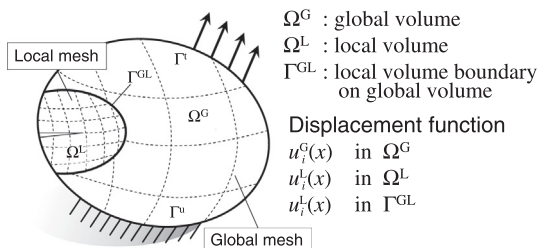


Fig. 1. Fundamental concept of relationship between global and local mesh in s-FEM.

area, and a full model is made. In each area, the displacement function is defined independently. In the overlapped area, the displacement is expressed by the summation of the displacements of each area. To maintain continuity at the boundary between the global and local areas  $\Gamma^{GL}$ , the displacement of the local area is assumed to be zero, as shown in the following equation:

$$u_i = \begin{cases} u_i^G & i \in \Omega^G - \Omega^L \\ u_i^G + u_i^L & i \in \Omega^L \\ u_i^t = 0 & i \in \Gamma^{GL} \end{cases} \quad (1)$$

The derivatives of the displacements can be written in the same way. These displacement functions are applied to the virtual work principle, as shown in Eq. (2), and the final matrix form of the s-FEM is obtained as shown in:

$$\begin{aligned} & \int_{\Omega^G} \delta u_{ij}^G D_{ijkl} u_{k,l}^G d\Omega + \int_{\Omega^L} \delta u_{ij}^L D_{ijkl} u_{k,l}^L d\Omega + \int_{\Gamma^{GL}} \delta u_{ij}^t D_{ijkl} u_{k,l}^t d\Omega \\ & + \int_{\Omega^L} \delta u_{ij}^L D_{ijkl} u_{k,l}^t d\Omega \\ & = \int_{\Gamma^{GL}} \delta u_i^t t_i d\Gamma^{GL} \end{aligned} \quad (2)$$

$$\begin{bmatrix} [K^{GG}] & [K^{GL}] \\ [K^{LG}] & [K^{LL}] \end{bmatrix} \begin{Bmatrix} \{u^G\} \\ \{u^L\} \end{Bmatrix} = \begin{Bmatrix} \{t^G\} \\ \mathbf{0} \end{Bmatrix} \quad (3)$$

where

$$\begin{aligned} [K^{GG}] &= \int_{\Omega^G} [B^G]^T [D^{GG}] [B^G] d\Omega & [K^{GL}] &= \int_{\Omega^L} [B^G]^T [D^{LL}] [B^L] d\Omega \\ [K^{LG}] &= \int_{\Omega^L} [B^L]^T [D^{LL}] [B^L] d\Omega & [K^{LL}] &= \int_{\Omega^L} [B^L]^T [D^{LL}] [B^L] d\Omega \end{aligned} \quad (4)$$

Note that  $[B^G]$  and  $[B^L]$  are the displacement–strain matrices defined in the global and local areas, respectively, and  $[D^{GG}]$  and  $[D^{LL}]$  are the stress–strain matrices described using the Young's modulus and Poisson's ratio.

In Eq. (3),  $[K^{LG}]^T = [K^{GL}]$ , and the stiffness matrix  $[D^{LL}]$  is symmetric. All of the matrices in Eq. (4) are calculated by numerical inte-

Download English Version:

<https://daneshyari.com/en/article/780775>

Download Persian Version:

<https://daneshyari.com/article/780775>

[Daneshyari.com](https://daneshyari.com)